Limits on cold-dark-matter candidates from deep underground detectors

T. K. Gaisser and G. Steigman
Bartol Research Foundation, University of Delaware, Newark, Delaware 19716

S. Tilav
Department of Physics, University of Delaware, Newark, Delaware 19716
(Received 2 July 1986)

Weakly interacting massive particles which are candidates for the dark mass in the halo of the Galaxy would be captured by the Sun, accumulate in the solar core, and annihilate. We present a systematic evaluation of the neutrino signal produced by such annihilations. Since most annihilations occur in the dense solar interior, only prompt neutrinos escape with sufficiently high energy to be readily observable in deep underground detectors. We find that existing underground experiments are capable of finding—or excluding—several possible cold-dark-matter candidates.

I. INTRODUCTION

Most of the mass in the Universe is dark, the nonluminous mass being detected by its gravitational effect. Since the origin of the unseen mass is unknown, various creatures from the particle-physics zoo have been proposed as candidates for the dark matter. These exotic particles may be grouped into a few broad categories: *hot*-dark matter (e.g., neutrinos with $m_\nu \sim$ tens of eV) will preserve perturbations on very large scales ($>$ clusters of galaxies), but erase those on smaller scales; *cold*-dark matter [e.g., massive ($>$ GeV) neutrinos, photinos, scalar neutrinos, axions, etc.] preserves perturbations on all scales; *warm*-dark matter (e.g., $\sim$ keV mass neutrinos or supersymmetric partners of the axions) is intermediate between the two, erasing perturbations on scales smaller than galaxies or groups of galaxies. Both warm- and cold-dark matter may collapse with galaxies and may dominate (over ordinary nucleons) the mass of the halos of galaxies. Since such weakly interacting massive particles (WIMP's) are nonluminous, few constraints to their properties are available. However, if present in sufficient abundance in the halo of the Galaxy, various *cold*-dark-matter candidates might be detectable through their annihilation radiation.[1] Such WIMP's would be accreted by the Sun,[2] accumulate in the solar core, and annihilate yielding a particularly striking signal of an excess of high-energy ($>$ GeV) ordinary neutrinos from the Sun observable in deep underground detectors. The concentration in the Sun of a WIMP X depends on its abundance in the Galaxy ($\rho_X/\rho_{\rm halo}$), its mass (m_X), and its cross sections for elastic scattering ($\sigma_{{\rm eff}\odot}$) and annihilation (σ_a). Some fraction of all annihilations will, via $X\bar{X}\rightarrow f\bar{f}\rightarrow\nu_i(\bar{\nu}_i)+$anything, yield detectable neutrinos of flavor i ($i=e,\mu,\tau$). Similar remarks apply, as well, to capture and annihilation in the Earth.[3]

It is our goal to present a systematic account of the expected neutrino fluxes and neutrino-induced event rates for several WIMP's which are cold-dark-matter candidates (Dirac and Majorana neutrinos, scalar neutrinos, and photinos). In particular, we will calculate the correct energy spectrum of the neutrinos at production and fold this with the correct energy dependence of the neutrino interaction cross section in the detector to compute the differential (with respect to E_ν), as well as the total event rate. Since the relevant annihilations occur in the dense interior of the Sun (or the Earth), only prompt neutrinos (e.g., from the decay of heavy-quark and -lepton flavors or from $X\bar{X}\rightarrow\nu_i\bar{\nu}_i$) will emerge with high energy. Charged pions and kaons will scatter in the dense interior ($\sim 10^2$ g cm^{-3}) of the Sun and thermalize, yielding ultimately mostly thermal photons and low-energy neutrinos typical of meson decay or capture at rest ($\sim$30 MeV for pions and muons and $\sim$230 MeV for kaons). Such low-energy neutrinos have cross sections too small to produce measurable interaction rates in present detectors for the annihilation rates of interest. For several of the WIMP's we shall consider, however, the couplings favor annihilation to heavy flavors and fluxes of relatively energetic prompt neutrinos are therefore quite large.

As a preliminary to our detailed calculations we first review the production and survival of WIMP's in the early Universe. Next we outline the galactic abundance, capture and annihilation rates of the various WIMP's, and calculate the fluxes and energy spectra of the resulting neutrinos. For each case we consider the branching ratios to each neutrino flavor as a function of m_X. Then we fold the neutrino fluxes with the appropriate cross sections to obtain the interaction rates. We apply our general results to several specific cases and conclude with a summary of the constraints (on m_X, m_S, ...) from present or future searches. To introduce the notation and to provide a qualitative preview of our results we begin with an outline of the calculation of the event rate expected in a deep underground detector.

II. OVERVIEW OF THE EVENT RATE

The flux at Earth of neutrinos of flavor i produced in $X\bar{X}$ annihilations in the Sun is

$$\phi_{\nu i}(E_\nu)=\phi_{\bar{\nu}i}(E_\nu)=\frac{\frac{1}{2}\dot{N}_X}{4\pi R^2}\sum_f B_{Xf}(m_X)B_{fi}g_{fi}(y)/m_X \ . \tag{1}$$

In (1), $\dot{N}_X$ is the rate of X captures in the Sun (the factor of $\frac{1}{2}$ accounts for the fact that two X's disappear in each annihilation so that the annihilation rate—in equilibrium—is one-half the capture rate); $R=1.5\times10^{13}$ cm [1 astronomical unit (AU)] is the Earth-Sun distance; $B_{Xf}(m_X)$ is the branching ratio of $X\bar{X}\to f\bar{f}$; B_{fi} is the branching ratio of $f\bar{f}\to\nu_i(\bar{\nu}_i)+$anything; $g_{fi}(y)$ is the normalized neutrino energy distribution where $y=E_\nu/m_X$ and for later use we define

$$N_{\nu i}(y)=\sum_f B_{Xf}(m_X)B_{fi}g_{fi}(y) \ , \tag{2a}$$

$$N_{\nu i}=\int N_{\nu i}(y)dy \ . \tag{2b}$$

In Sec. IV we compute the capture rate $\dot{N}_X$; we will find

$$\dot{N}_{X\odot}\approx(3.6\times10^{29}/m_X)(\sigma_{\rm eff}/\sigma_c)_\odot(\rho_X/\rho_{\rm halo})(v_{\rm halo}/v_X) \ ,$$

where $\sigma_{\rm eff\odot}$ is the effective cross section for elastic scattering of X's with the nuclei in the Sun and $\sigma_{c\odot}$ is a critical cross section corresponding roughly to one scattering per traversal of the Sun ($\sigma_{c\odot}=R_\odot{}^2m_{\rm H}/M_\odot\approx4\times10^{-36}$ cm^2). ρ_X and v_X are the mass density and velocity of X's in the halo of our Galaxy; for the Galaxy, $\rho_{\rm halo}\approx0.3$ GeV cm^{-3} and $v_{\rm halo}\approx300$ km sec^{-1}; here and elsewhere in this paper m_X is in GeV.

Roughly, then, we expect a differential flux and a total flux of neutrinos of type i whose magnitudes are

$$\phi_{\nu i}(E_\nu)\approx(64/m_X)[N_{\nu i}(y)/m_X](\sigma_{\rm eff}/\sigma_c)_\odot(\rho_X/\rho_{\rm halo})(v_{\rm halo}/v_X) \ , \tag{3a}$$

$$\phi_{\nu i}\approx(6.4/m_X)(N_{\nu i}/0.1)(\sigma_{\rm eff}/\sigma_c)_\odot(\rho_X/\rho_{\rm halo})(v_{\rm halo}/v_X) \ . \tag{3b}$$

To estimate the event rates we must fold $\phi_{\nu i}$ with the neutrino-nucleon cross section. For the charged-current interactions of energetic ($>$ GeV) ν_e and ν_μ,

$$\sigma_\nu(E_\nu)+\sigma_{\bar{\nu}}(E_\nu)\approx1\times10^{-38}E_\nu\ ({\rm GeV})\ {\rm cm}^2 \ . \tag{4}$$

Here and throughout the paper we have used only charged-current interactions to estimate event rates because in these interactions in principle all of the neutrino energy is detectable. The neutral-current interactions will increase the total event rate by about one-third, but these events will be more difficult to distinguish from background because of the variable missing energy. The procedure we adopt gives a conservative estimate of the dark-matter-induced event rate.

The event rate per kt yr GeV (kt represents kiloton) is $R_i(E_\nu)\approx1.9\times10^{40}(\sigma_\nu+\sigma_{\bar{\nu}})\phi_\nu(E_\nu)$ so that

$$R_i(E_\nu)\approx1.2\times10^4[yN_{\nu i}(y)/m_X](\sigma_{\rm eff}/\sigma_c)_\odot(\rho_X/\rho_{\rm halo})(v_{\rm halo}/v_X) \ , \tag{5a}$$

$$R_i=\int R_i(E_\nu)dE_\nu\approx400(N_{\nu i}/0.1)(\sigma_{\rm eff}/\sigma_c)_\odot(\rho_X/\rho_{\rm halo})(v_{\rm halo}/v_X) \ . \tag{5b}$$

In (5) we have used the result that, for prompt, three-body semileptonic decays of f,

$$\langle y\rangle=\langle E_\nu\rangle/m_X=\int yN_{\nu i}(y)dy/N_{\nu i}\approx\tfrac{1}{3} \ . \tag{6}$$

Note that if $\sigma_{\rm eff\odot}$ were of order $\sigma_{c\odot}$, the predicted event rate would be enormous; typically, $\sigma_{\rm eff\odot}$ is $\frac{1}{100}$ to $\frac{1}{40}$ of $\sigma_{c\odot}$ so that, for $N_{\nu i}\approx0.1$, a few to ~10 events per kiloton year is expected.

The rates predicted for WIMP annihilation in the Sun should be compared to the atmospheric background. The total atmospheric background—from all directions and integrated over all energies—yields an expected rate in the large underground detectors of order 100 events per kiloton year.[4] The signal-to-background ratio can be enhanced by realizing that the background is concentrated at low energy and by exploiting the angular resolution. For example, for $\gtrsim$ GeV ν_e and ν_μ, charged-current interactions have an overall angular resolution of $\lesssim35°$ so that the background would be reduced by a factor of $\gtrsim10$. An event rate—from WIMP annihilation in the Sun—of a few per kiloton year should be detectable. Thus the deep underground detectors are capable of discovering—or excluding—WIMP's which are cold-dark-matter candidates.

III. SURVIVAL OF WIMP's IN THE EARLY UNIVERSE

The production, destruction, and survival of particles during the early evolution of the Universe was first analyzed by Zeldovich[5] and by Chiu.[5] All subsequent work has been to extend and generalize the Zeldovich-Chiu analysis (see, for example, Steigman[5] and references therein). At high temperatures the production and annihilation rates are rapid compared to the universal expansion rate and equilibrium is established and maintained ($n_X=n_{\rm eq}$). For WIMP's, when $T\lesssim m_X$, $n_{\rm eq}\propto T^3x^{3/2}e^{-x}$ where T is the radiation temperature and $x\equiv m_X/T$. When the temperature drops to a critical value $T=T_*$, deviations from equilibrium occur ($n_X>n_{\rm eq}$) because the interaction rates are too slow to keep up with expansion rate. For $T<T_*$, annihilation dominates and the abundance of X's decreases until the density of X's is so low that no further annihilations occur—the X's "freeze-out."

The critical temperature T_* (when deviations from equilibrium begin) is reached when the annihilation rate is x_* times the expansion rate (Hubble parameter): $\Gamma_{\rm ann}{}^*=x_*H_*$ (Steigman[5]). x_* is the solution of

$$x_*{}^{1/2}e^{x_*}=5\times10^{34}g_Xm_X\langle\sigma_a v\rangle_*g_*{}^{-1/2} \ . \tag{7}$$

In (7), g_X and m_X (in GeV) are the number of spin states and mass of X, $\langle \sigma_a v \rangle_*$ (in $\mathrm{cm^3\,sec^{-1}}$) is the thermally averaged annihilation rate coefficient, averaged over initial states and summed over all final states; g_* is the effective number of relativistic degrees of freedom at T_* (see Steigman[5]). The final number of X's in a comoving volume is smaller than the number present at T_* by a factor $x_*(N_{Xf}/N_{X*} \approx x_*^{-1})$; for weakly interacting particles, $x_* \approx 20$.

For symmetric relics,[5]

$$N_X/N_\gamma = N_{\bar{X}}/N_\gamma \approx 5\times 10^{-34} x_* (m_X \langle \sigma_a v \rangle_* g_*^{1/2})^{-1} . \tag{8}$$

The present mass density in X's may be written in terms of the present critical density: $\rho_X = \Omega_X \rho_c$, $\rho_c = 1\times 10^{-5}(H_0/100)^2$ GeV cm^{-3} where $\rho_X = m_X(n_X + n_{\bar{X}})$:

$$\Omega_X h_{1/2}^2 = (1.9\times 10^{-26}/\langle \sigma_a v \rangle_*)(x_*/20)(64/g_*)^{1/2} . \tag{9}$$

In (9) we have written the Hubble parameter as $H_0 = 50 h_{1/2}$ km sec^{-1}Mpc^{-1}. As Eq. (9) shows, a WIMP with a typical weak annihilation cross section can close the Universe (i.e., $\Omega_X h_{1/2}^2 \approx 1$ for $\langle \sigma_a v \rangle \approx 2\times 10^{-26}$ cm^{3}sec^{-1}).

Care must be taken in applying these results. Strictly speaking they have been derived for s-wave annihilation of particles with short-range forces ($\sigma_a \propto v^{-1}$). Sherrer and Turner[6] have considered the case that $\sigma_a v \propto v^{2n}$. Up to logarithmic factors, x_* is unchanged but the right-hand sides of (8) and (9) must be multiplied by $(n+1)$ in the general case. For the particles we will consider subsequently only s- and p-wave contributions are relevant. If we write $\langle \sigma_a v \rangle_* = a + b x_*^{-1}$, then (see also Ellis *et al.*[7] and Kolb and Olive[7])

$$\Omega_X h_{1/2}^2 = (1.9\times 10^{-26}/\langle \sigma_a v \rangle_*)(x_*/20)(64/g_*)^{1/2}(b + a x_*)(b/2 + a x_*)^{-1} . \tag{10}$$

Majorana particles require special attention. In averaging over identical particles in the initial state, $\langle \sigma_a v \rangle$ should be divided by 2 to avoid double counting. However, this can be ignored if it is realized that for Majorana particles, two X's disappear in each annihilation[7] (i.e., $\langle \sigma_a v \rangle_{\mathrm{eff}} = 2\times \frac{1}{2}\langle \sigma_a v \rangle = \langle \sigma_a v \rangle$). Since $X = \bar{X}$, $\rho_X = m_X n_X$ (not $2 m_X n_X$), Eq. (10) must be divided by 2 for Majorana particles.

Superficially, it might appear from (10) that $\Omega_X h_{1/2}^2$ is independent or, only weakly dependent, on the mass of the WIMP. This is misleading. For most examples of interest, $\langle \sigma_a v \rangle \propto m_X^2$ so that $\Omega_X h_{1/2}^2 \propto m_X^{-2}$. In general, there will be a minimum value of the mass, below which the WIMP density is too high ($\Omega_X h_{1/2}^2 > 1$). There may also be a maximum value of m_X, above which WIMP's are less important than ordinary nucleons: $\Omega_X < \Omega_N$. Big-bang nucleosynthesis[8] constrains the nucleon density to lie in the range $0.04 < \Omega_X h_{1/2}^2 < 0.16$.

IV. CAPTURE OF COLD-DARK-MATTER CANDIDATES (REF. 2)

Consider some cold-dark-matter candidate X which collapsed along with the Galaxy. During the dynamical collapse, violent relaxation[9] would have thermalized the phase-space distribution of the X's yielding $n_X(v) \propto (v^2/v_X^3)\exp(-3v^2/2v_X^2)$ where $v_X = v_{\mathrm{halo}} \approx 300$ km sec^{-1} is the average velocity of the X's. If $\rho_X = m_X n_X$ is the density of X's in the Galaxy then the differential flux (per unit velocity interval) is $\sim v\rho_X(v)/m_X$; the flux of X's with $v < v_*$ is, for $v_* < v_X$, $\sim(\rho_X/m_X)(v_*^4/v_X^3)$ where ρ_X is the total density of X's in the Galaxy. In passing through the Galaxy, the X's will encounter massive bodies (e.g., the Sun, the Earth, etc.) and, if v_* is less than the escape velocity ($v_{\mathrm{esc}}^2 = 2GM/R$) gravity will focus the X's towards those objects. There is a critical impact parameter $b_* = R v_{\mathrm{esc}}/v_*$ such that for $b < b_*$, the X's will pass through the object. For a target of mass M and radius R, the number of X's passing through per unit time is $\sim(\rho_X/m_X)(v_*^4/v_X^3)b_*^2 \sim (\rho_X/m_X)R^2(v_{\mathrm{esc}}^2 v_*^2/v_X^3)$. In passing through the object the X may undergo an elastic scattering which, if v_* is sufficiently small, may leave the X bound. If the "optical depth" of the object to X's is small, the probability of such a collision is $\sim(M/R^2)\sigma_{\mathrm{eff}}/m_{\mathrm{H}}$ where σ_{eff} is an appropriately mass-weighted scattering cross section and m_{H} is the proton mass. The rate at which X's are captured is thus

$$\dot{N}_X \sim (\rho_X/m_X)(M/m_{\mathrm{H}})(v_{\mathrm{esc}}^2 v_*^2/v_X^3)\sigma_{\mathrm{eff}} . \tag{11}$$

For the Sun, $v_{\mathrm{esc}\odot} \approx 620$ km sec$^{-1} > v_X$ so that $v_* \approx v_X$ and $\dot{N}_{X\odot} \propto (m_X v_X)^{-1}\sigma_{\mathrm{eff}\odot}$. From Press and Spergel,[2]

$$\dot{N}_{X\odot}\,(\mathrm{sec}^{-1}) = 8.8\times 10^{64}(\sigma_{\mathrm{eff}\odot}/m_X)(\bar{\rho}_X/\bar{v}_X) . \tag{12}$$

In (12) we have written $\rho_X = \bar{\rho}_X \rho_{\mathrm{halo}} \approx 0.3\bar{\rho}_X$ (GeV cm^{-3}) and $\bar{v}_X = v_X/v_{\mathrm{halo}} \approx v_X/300$ km sec^{-1}. The effective cross section for scatterings in the Sun is

$$\sigma_{\mathrm{eff}\odot} = X_{\mathrm{H}} \sum_i (n_i/n_{\mathrm{H}})\sigma_{Xi} , \tag{13}$$

where X_{H} is the hydrogen mass fraction (≈ 0.7), n_i/n_{H} is the abundance of nucleus i (by number with respect to hydrogen) and σ_{Xi} is the scattering cross section. In the following we will adopt $n_{\mathrm{He}}/n_{\mathrm{H}} = 0.1$ and follow Cameron[10] for the abundances of the other nuclei.

For the Earth, the results are quite different. Since $v_{\mathrm{esc}\oplus} \approx 11$ km sec$^{-1} \ll v_X$, only very slow moving X's are kinematically capable of being captured in a single scatter with a nucleus (essentially iron) in the Earth. In this case, $v_*^2 \approx \alpha_\oplus v_{\mathrm{esc}\oplus}^2$ where[2]

$$\alpha_\oplus = 2 b_\oplus m_X m_i (m_X^2 + m_i^2)^{-1} ; \tag{14}$$

$b_\oplus$ is a numerical coefficient which depends on the density distribution of the Earth; Krauss, Srednicki, and

Wilczek[3] estimate $b_\oplus \approx 1.7$. For $i=$Fe and $m_X \ll m_{\rm Fe}$, $\alpha_\oplus \approx 3.4 m_X/m_{\rm Fe}$. Comparing with (11) we see that $\dot{N}_{X\oplus} \sim v_X^{-3}\sigma_{{\rm eff}\oplus}$. Limiting ourselves to the iron core of the Earth,[3] we find

$$\dot{N}_{X\oplus} \approx 4.6\times 10^{49}(\bar{\rho}_X/\bar{v}_X{}^3)\sigma_{X{\rm Fe}}({\rm sec}^{-1}) . \quad (15)$$

If X, indeed, is the WIMP which accounts for the dark mass in the Universe, we expect that $\bar{\rho}_X = 1$. However, even if X is cosmologically unimportant, there may be detectable events from its capture and annihilation in the Sun and/or Earth. If $\Omega_X < \Omega_N^{\rm min}$ we will assume that $\bar{\rho}_X = \Omega_X/\Omega_N^{\rm min}$. From Yang *et al.*[8] and Boesgaard and Steigman,[8] we adopt $\Omega_N^{\rm min} h_{1/2}{}^2 = 0.04$ so that

$$\bar{\rho}_X = 1 \quad \text{for } \Omega_X h_{1/2}{}^2 \geq 0.04 , \quad (16a)$$

$$\bar{\rho}_X = \Omega_X h_{1/2}{}^2/0.04 \quad \text{for } \Omega_X h_{1/2}{}^2 \leq 0.04 . \quad (16b)$$

V. ANNIHILATION OF COLD-DARK-MATTER CANDIDATES

Once captured by the Sun, X's will come to thermal equilibrium and sink to the solar core (for $m_X > m_{\rm H}$). The scale radius of the region in which the X's are concentrated is[2]

$$r_X \approx 5\times 10^9 m_X{}^{-1/2}\ {\rm cm} \ll R_\odot \approx 7\times 10^{10}\ {\rm cm} . \quad (17)$$

With time, the X concentration will increase until the density is high enough for $X\bar{X}$ annihilation to occur. In equilibrium, the capture rate will be twice the annihilation rate (an X and $\bar{X}$ disappear in each annihilation). A steady state will be achieved if the time to reach equilibrium is short compared to the age of the Sun. The time scale to reach equilibrium is

$$t_{\rm eq}{}^{-1} = (2\dot{N}_{X\odot}\langle\sigma_a v\rangle_\odot/V_\odot)^{1/2} , \quad (18)$$

where $V_\odot \approx 3\times 10^{31} m_X{}^{-3/2}$ cm^3 is the effective volume[2] and $\langle\sigma_a v\rangle_\odot$ is the annihilation rate coefficient appropriate to the temperature of the solar core. For the specific candidates discussed below, we have compared $t_{\rm eq}$ to $t_\odot$ ($\approx 1.4\times 10^{17}$ sec) and find that in all cases of interest $t_{\rm eq} \ll t_\odot$.

Among the annihilation products will be the "ordinary," light neutrinos (ν_e, ν_μ, ν_τ). If, in a typical annihilation $N_{\nu i}(E_\nu)dE_\nu$ neutrinos of type i are produced with energy between E_ν and $E_\nu + dE_\nu$, then the differential flux of such neutrinos at Earth is

$$\phi_{i\odot}(E_\nu) = \frac{\frac{1}{2}\dot{N}_{X\odot}N_{\nu i}(E_\nu)}{4\pi(1\ {\rm AU})^2} \approx 1.6\times 10^{37}(\sigma_{{\rm eff}\odot}/m_X)(\rho_X/\bar{v}_X)N_{\nu i}(E_\nu)\ ({\rm cm}^2\,{\rm sec}\,{\rm GeV})^{-1} . \quad (19)$$

It is of interest to compare the above flux with that expected from capture in the Earth.[3] It follows from (12) and (15) that

$$\phi_\odot/\phi_\oplus \sim 3.5\times 10^6(\bar{v}_X{}^2/m_X)(\sigma_{{\rm eff}\odot}/\sigma_{X{\rm Fe}}) . \quad (20)$$

For Dirac neutrinos and for scalar neutrinos coherent scattering from iron nuclei in the core of the Earth may be significant.[3] As we shall see below, however, for all m_X, $\phi_\odot$ exceeds $\phi_\oplus$ by more than an order of magnitude [D. Seckel (private communication)].

VI. EVAPORATION

It must be noted that very light X's will evaporate from the Sun before they annihilate. Below a critical mass $m_{X,{\rm evap}}$, there is a cutoff to the flux of annihilation neutrinos. In their original discussion of WIMP's in the Sun, Steigman *et al.*[11] estimated $m_{X,{\rm evap}} \approx 4$ GeV. Spergel and Press[2] have discussed evaporation in greater detail and find $m_{X,{\rm evap}} \approx 4.1$ GeV.

It is convenient to identify two separate contributions to the evaporation rate $t_{\rm evap}{}^{-1}$ [Ref. 2 and Spergel and Press (private communication)]. A WIMP in the high-velocity tail of the thermal distribution may scatter from a "thermal" nucleus and gain sufficient energy to escape. In addition, a thermal WIMP may be kicked out of the Sun after scattering from a high-velocity (superthermal) nucleus. We have evaluated both contributions to the total evaporation rate and have found that the first process always dominates. Following Spergel and Press[2] but correcting several misprints, we find

$$t_{\rm evap} \approx 2^{1/2}(15.8)^{-5/4}\left[\frac{\sigma_{\rm crit}}{\sigma_{\rm eff}}\right]_\odot \left[\frac{m_X}{m_{\rm H}}\right] \times GM_\odot\left[\frac{m_{\rm H}}{kT}\right]^{3/2}\exp\left[7.9\frac{m_X}{m_{\rm H}}\right] , \quad (21)$$

where the escape velocity from the solar core[2] is $v_{\rm esc}{}^2 \approx 15.8\ {\rm kT}/m_{\rm H}$ and $\sigma_{\rm crit} = R_\odot{}^2(M_\odot/m_{\rm H})^{-1}$. Below, we will evaluate $t_{\rm evap}$ for each of our candidate particles. However, since the exponential in (21) dominates we will find $m_{X,{\rm evap}} \approx 3$ GeV for all cases. First, though, let us define $m_{X,{\rm evap}}$ more precisely.

The evolution of WIMP's in the Sun is described by

$$\frac{dN}{dt} = \dot{N} - 2N^2\left[\frac{\langle\sigma_a v\rangle}{V}\right] - \frac{N}{t_{\rm evap}} . \quad (22)$$

For convenience we have dropped the subscripts X and $\odot$. The first term on the right-hand side of (22) accounts for captures, the second term accounts for annihilations, and the third term accounts for evaporations. The solution to (22) at present ($t = t_\odot$) is

$$\frac{N}{N_{\rm eq}} = \frac{1-\exp[-(\eta_1-\eta_2)t_\odot/t_{\rm eq}]}{\eta_1\exp[-(\eta_1-\eta_2)t_\odot/t_{\rm eq}]-\eta_2} , \quad (23)$$

where $t_{\rm eq}$ is given in (18), $N_{\rm eq} = \dot{N}t_{\rm eq}$ is the equilibrium number of WIMP's in the absence of evaporation and

$$\eta_{1,2} = -\epsilon \pm (\epsilon^2+1)^{1/2} , \quad \epsilon = t_{\rm eq}/2t_{\rm evap} . \quad (24)$$

For heavy particles evaporation is unimportant ($t_{eq} \ll t_{evap}$, $\epsilon \to 0$) so that, for $t_{eq} < t_\odot$, $N \approx N_{eq}$. In contrast, for light particles evaporation will dominate ($t_{evap} \ll t_{eq}, \epsilon \to \infty$) and, for $t_{evap} < t_{eq} < t_\odot$, the steady-state number of WIMP's in the Sun is reduced from its value in the absence of evaporation

$$N/N_{eq} \approx t_{evap}/t_{eq} \ . \tag{25}$$

Later we evaluate t_{evap} and t_{eq} as a function of m_X for our candidate particles. $m_{X,evap}$ is defined as that value of m_X such that evaporation reduces the flux of annihilation neutrinos by a factor of 2: $(N/N_{eq})^2 = \frac{1}{2}$ at $m_X = m_{X,evap}$.

VII. BRANCHING RATIOS AND EVENT RATES

For energetic neutrinos from $X\bar{X}$ annihilations to $f\bar{f}$ there are two energy distributions. If $f = \nu$, the neutrinos are monoenergetic with $E_\nu = m_X$. For $X\bar{X} \to Q\bar{Q}$ (where $Q = c$ or b), followed by semileptonic decay of the heavy quarks, the energy distribution of the neutrinos can be adequately described by the spectator quark model.[12] The lepton distributions, including QCD corrections, have been worked out by Cabibbo, Corbo, and Maiani[13] for $c \to sl\nu$ and by Altarelli, Cabibbo, Corbo, Maiani, and Martinelli[13] for $b \to cl\nu$. Although radiative QCD corrections change the magnitude significantly, they change the *shape* of distribution only near the end point. Since, in the present application, only the shape is relevant, we employ the appropriate uncorrected shape. For similar reasons we are justified in ignoring the Fermi momentum of the heavy quark inside its hadron. In this approximation the neutrino distributions are the same as those in τ decay (and in muon decay) with appropriate changes of mass. In the rest frame of the c, the momentum distribution of the neutrino from $c \to sl\nu$ is

$$g_{c\nu}(x) \propto 12x^2(x_m - x)^2/(1-x) \ , \tag{26}$$

where $x_m = 1 - (m_s/m_c)^2$ and $x = 2E_\nu^*/m_c$ where E_ν^* is the neutrino energy in the rest frame of the c. For $b \to cl\nu$ the corresponding distribution is

$$g_{b\nu}(x) \propto 2x^2(x_m - x)^2(1-x)^{-3} \times [(1-x)(3-2x) + (1-x_m)(3-x)] \ , \tag{27}$$

where, now, $x_m = 1 - (m_c/m_b)^2$ and $x = 2E_\nu^*/m_b$. The ν_τ distribution in τ decay is of the same form as in (27). For the distribution $g_{c\nu}$, the mean energy of the neutrino is $\simeq 0.3 m_X$ whereas for $g_{b\nu}$, the mean energy is $\simeq 0.35 m_X$.

If $B_{Xf}(m_X)$ is the branching ratio for $X\bar{X} \to f\bar{f}$ and B_{fi} that for $f \to \nu_i$ + anything, then the differential number of neutrinos of type i with (laboratory) energy E_ν is given in Eq. (2). For use in Eq. (2) the distributions in Eqs. (26) and (27) must first be transformed into the laboratory frame. In terms of the variable $y = E_\nu/m_X$ they are, respectively, $2 - 6y^2 + 4y^3$ and $\frac{5}{3} + \frac{4}{3}y^3 - 3y^2$ in the approximation $x_m = 1$.

Only prompt neutrinos from the decay of τ, c, and b (and, occasionally from $X\bar{X} \to \nu\bar{\nu}$) are sufficiently energetic to be detectable. τ leptons can decay to ν_τ plus $e(\nu_e)$ or $\mu(\nu_\mu)$ or $u(d)$ quarks. Accounting for the three colors of the quarks,

$$B_{\tau\nu_e} = \tfrac{1}{5} \ , \quad B_{\tau\nu_\mu} = \tfrac{1}{5} \ , \quad B_{\tau\nu_\tau} = 1 \ . \tag{28}$$

Charm quarks will decay to strange quarks plus $e(\nu_e)$, $\mu(\nu_\mu)$, or $u(d)$ quarks. For charm decay,

$$B_{c\nu_e} = \tfrac{1}{5} \ , \quad B_{c\nu_\mu} = \tfrac{1}{5} \ , \quad B_{c\nu_\tau} = 0 \ . \tag{29}$$

(The observed semileptonic branching ratio for D^0 decay is significantly less than for $D^\pm$ decay, so use of these naive branching ratios may overestimate the contribution via charm channels to some extent.) More channels are available in the decay of the heavier b quark: $u(d)$, $c(s)$, $e(\nu_e)$, $\mu(\nu_\mu)$, $\tau(\nu_\tau)$:

$$B_{b\nu_e} = \tfrac{1}{9} \ , \quad B_{b\nu_\mu} = \tfrac{1}{9} \ , \quad B_{b\nu_\tau} = \tfrac{1}{9} \ . \tag{30}$$

Note that in (30) we have only included "direct" ν production; ν production from the subsequent decays of c and τ will be included separately—this separation is necessary because of the different distributions of neutrino energy from b, c, and τ decay. For ν_e and ν_μ from c and τ decay, $\langle y \rangle = 0.3$; for all νs from b decay and ν_τ from τ decay, $\langle y \rangle = 0.35$.

The branching ratios B_{Xf} depend on the mass and the nature of the annihilating WIMP and will be given when we discuss each case in its turn. We may now assemble our results to compute the expected flux and event rate from energetic neutrinos produced in the annihilation of WIMP's from the halo of our Galaxy which have been captured by the Sun.

VIII. FLUXES AND EVENT RATES

In the absence of evaporation the differential flux of neutrinos of type i and energy E_ν produced by WIMP annihilation in the Sun is given by (19) where $N_{\nu i}(E_\nu)$ is given by (2). To account for possible evaporation, we should multiply (19) by $(N/N_{eq})^2$ (see Sec. VI):

$$\phi_{i\odot}(E_\nu) = 1.6 \times 10^{37} \left[\frac{\sigma_{eff\odot}}{m_X}\right] \left[\frac{\bar{\rho}_X}{\bar{v}_X}\right] \left[\frac{N}{N_{eq}}\right]^2 N_{\nu i}(E_\nu) \ (\text{cm}^2 \text{sec GeV})^{-1} \ . \tag{19'}$$

Since there are $\sim 1.9 \times 10^{40}$ nucleon sec in 1 kt yr, the differential event rate corresponding to the above flux is

$$R_i(E_\nu) = 3.0 \times 10^{39} \sigma_{eff\odot} \left[\frac{\bar{\rho}_X}{\bar{v}_X}\right] \left[\frac{N}{N_{eq}}\right]^2 \left[\frac{E_\nu}{m_X}\right] N_{\nu i}(E_\nu) \ (\text{kt yr GeV})^{-1} \ , \tag{31}$$

where we have used the neutrino-nucleon cross section in (4). The total event rate, integrated over E_ν, is

$$R_i = 3.0\times 10^{39}\sigma_{\text{eff}\odot}\left[\frac{\bar{\rho}_X}{\bar{v}_X}\right]\left[\frac{N}{N_{\text{eq}}}\right]^2\langle y\rangle N_{\nu i} . \quad (32)$$

In fact, the above is strictly applicable only to ν_e and ν_μ. For ν_τ-nucleon charge-current interactions one must account for the threshold energy (~ 3.5 GeV) due to the large τ mass. The corresponding ν_τ-nucleon cross section[14] must be used to compute an "effective" $\langle y(m_X)\rangle$ in place of $\langle y\rangle$:

$$\langle y(m_X)\rangle = 1\times 10^{38}\int_{y_{\text{th}}}^{y_{\max}} g(y)[\sigma_{\nu_\tau}(E_\nu)+\sigma_{\bar{\nu}_\tau}(E_\nu)]dy/E_\nu , \quad (33)$$

where $y_{th}=(m_\tau/m_X)[1+m_\tau/(2m_{\text{H}})]$ and $y_{\max}=(1+\beta)/2$ where β is the velocity of the parent τ lepton. $\langle y(m_X)\rangle$ is shown in Fig. 1; only for very large values of m_X does $\langle y(m_X)\rangle$ approach its asymptotic value of 0.35. For ν_τ produced directly ($X\bar{X}\to\nu_\tau\bar{\nu}_\tau$), $g(y)=\delta(y-1)$ and we must use $\langle\tilde{y}(m_X)\rangle$, where

$$\langle\tilde{y}(m_X)\rangle = 1\times 10^{38} m_X{}^{-1}[\sigma_{\nu_\tau}(m_X)+\sigma_{\bar{\nu}_\tau}(m_X)] . \quad (34)$$

$\langle\tilde{y}(m_X)\rangle$ is shown in Fig. 1; only for very large m_X does $\langle\tilde{y}(m_X)\rangle$ approach its asymptotic value of 1. For ν_τ then, $\langle y\rangle N_{\nu i}$ is replaced by

$$B_{X\nu_\tau}(m_X)\langle\tilde{y}(m_X)\rangle+\sum_f B_{Xf}(m_X)B_{f\nu_\tau}\langle y(m_X)\rangle . \quad (35)$$

We now proceed to consider four candidate WIMP's: Dirac neutrinos, Majorana neutrinos, scalar neutrinos, and photinos. For each WIMP we will calculate the relic abundance Ω_X (Sec. III) as a function of m_X and compare with Ω_N; for $\Omega_X h_{1/2}{}^2\geq 0.04$, $\bar{\rho}_X=1$ whereas, for $\Omega_X h_{1/2}{}^2\leq 0.04$, $\bar{\rho}_X=\Omega_X h_{1/2}{}^2/0.04$. To compute Ω_X we will need to know $\langle\sigma_a v\rangle_*$, the annihilation rate coefficient (as a function of m_X) when $T_*\approx m_X/x_*$, where $x_*\approx 20$. Next, we will calculate the rate for capture by the Sun (and/or Earth) and the time scales to reach equilibrium (t_{eq}) and for evaporation (t_{evap}) so that we may evaluate the flux (19′) and the predicted event rate [(31) and (32)]. By requiring that the density of relic WIMP's not be too large ($\Omega_X h_{1/2}{}^2\lesssim 1$) and that the event rate not be too large, we will constrain the masses of such particles.

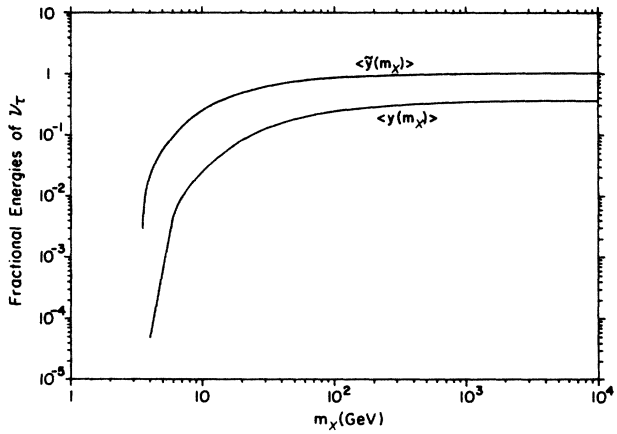

FIG. 1. The effective average fractional energies of ν_τ (see the text) as a function of the mass of the annihilating particle; see Eqs. (33) and (34).

A. Dirac neutrinos

In general, massive neutrinos can annihilate to lighter leptons via Z^0 or $W^\pm$ exchange. The cross section for Dirac neutrino ($X\equiv\nu_D$) annihilation was derived by Kane and Kani[15] on the assumption that the charged current interactions are Cabibbo suppressed:

$$\sigma_a v = \frac{G_F'{}^2}{4\pi}\sum_f (1-m_f{}^2/m_{\nu_D}{}^2)^{1/2}\left[(C_{Vf}{}^2+C_{Af}{}^2)[2m_{\nu_D}{}^2+\tfrac{1}{6}(7m_{\nu_D}{}^2-m_f{}^2)v^2]+(C_{Vf}{}^2-C_{Af}{}^2)m_f{}^2\left[1+\frac{v^2}{2}\right]\right] , \quad (36a)$$

where

$$G_F' = G_F\left\{\left[1-\left[\frac{2m_\nu}{m_Z}\right]^2\right]^2+\left[\frac{\Gamma_z}{m_Z}\right]^2\right\}^{-1} . \quad (36b)$$

In (36), G_F is the Fermi constant (1.16×10^{-5} GeV^{-2}), $\Gamma_z\approx 3$ GeV is the Z^0 width and $m_Z\approx 93$ GeV is the Z^0 mass; f is any fermion with $m_f<m_{\nu_D}$ (three colors of quarks are counted); v is the $\nu_D-\bar{\nu}_D$ relative velocity; for $f=\nu_e,\nu_\mu,\nu_\tau$, $-C_A=C_V=\frac{1}{2}$; for $f=e,\mu,\tau$, $C_A=+\frac{1}{2}$, $C_V=-0.048$; for u,c, $C_A=-\frac{1}{2}$, $C_V=0.199$; for d,s,b, $C_A=\frac{1}{2}$, $C_V=-0.349$ (we have used $\sin^2\theta_W=0.226$). It is clear that at low energy ($v^2\ll 1$), s-wave annihilation dominates so that $\langle\sigma_a v\rangle_*\approx\langle\sigma_a v\rangle_\odot=\langle\sigma_a v\rangle$ where

$$\langle\sigma_a v\rangle = \frac{G_F'{}^2}{4\pi}m_{\nu_D}{}^2\sum_f (1-m_f{}^2/m_{\nu_D}{}^2)^{1/2}[2(C_{Vf}{}^2+C_{Af}{}^2)+(C_{Vf}{}^2-C_{Af}{}^2)m_f{}^2/m_{\nu_D}{}^2] . \quad (37)$$

We have used the above cross section to find the density of relic—*stable*—massive Dirac neutrinos. In Fig. 2 we show $\Omega_{\nu_D}h_{1/2}{}^2$ as a function of m_{ν_D}. For relatively small m_{ν_D}, $\Omega_{\nu_D}h_{1/2}{}^2=1$ (0.04) for $m_{\nu_D}=3.6$ (15) GeV. The dip in $\Omega_{\nu_D}h_{1/2}{}^2$ reflects the resonant behavior of the annihilation cross section. For much larger values of the neutrino mass, $\sigma_a v \propto m_{\nu_D}{}^{-2}$ so that $\Omega_{\nu_D}h_{1/2}{}^2$ increases again.

The elastic scattering cross section for Dirac neutrinos will receive contributions from the coherent vector and spin-dependent axial-vector couplings. The axial term dominates the scattering from protons.[16] Neutrinos scatter coherently from even-even nuclei since the axial contribution is absent. Even for heavy nuclei with spin the axial contribution is small and the vector coupling dominates. For the scattering of Dirac neutrinos by a nucleus of mass m_n with Z protons and N neutrons, Goodman and Witten[17] find

$$\sigma_{\nu n}=\frac{G_F{}^2}{2\pi}\overline{Y}^2\left[\frac{m_n m_\nu}{m_n+m_\nu}\right]^2[N-Z(1-4\sin^2\theta_W)]^2\ , \quad (38)$$

where $\overline{Y}=\frac{1}{2}(Y_L+Y_R)$ is the average hypercharge of the left- and right-handed components of the neutrino. For scattering from protons[16]

$$\sigma_{\nu p}=\frac{2G_F{}^2}{\pi}\left[\frac{m_p m_\nu}{m_p+m_\nu}\right]^2[(C_V-1)^2+3(C_A-1)^2]\ , \quad (39)$$

where, for protons $C_V=\frac{1}{2}+\sin^2\theta_W\approx 0.954$ and $C_A=\frac{1}{2}$. For Dirac neutrinos, $Y_L=-1$ and $Y_R=0$ so that $\overline{Y}=-\frac{1}{2}$. The effective cross section for Dirac neutrinos scattering in the Sun is [see Eq. (13)]

$$\sigma_{\text{eff}\odot}=0.7\frac{G_F{}^2}{8\pi}\Gamma_{\nu_D}\approx 1.5\times 10^{-39}\Gamma_{\nu_D}\ \text{cm}^2\ , \quad (40a)$$

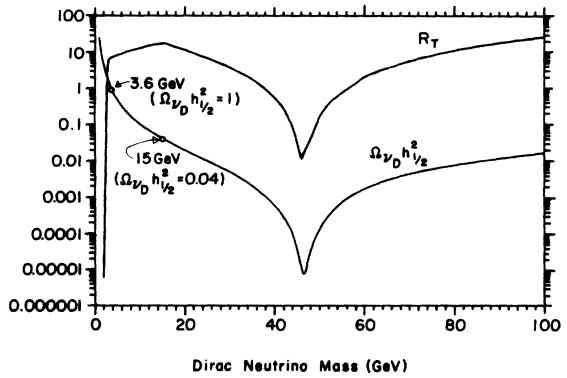

FIG. 2. The event rate (R_T) per kiloton year for neutrinos from the annihilation of heavy Dirac neutrinos captured by the Sun. Also shown is the relic density ($\Omega_{\nu_D}h_{1/2}{}^2$) of such Dirac neutrinos.

where

$$\Gamma_{\nu_D}=16\left[\frac{m_{\rm H}m_\nu}{m_{\rm H}+m_\nu}\right]^2[(2\sin^2\theta_W-\tfrac{1}{2})^2+\tfrac{3}{4}]+\sum_i\left[\frac{n_i}{n_{\rm H}}\right]\left[\frac{m_i m_\nu}{m_\nu+m_i}\right]^2[N_i-Z_i(1-4\sin^2\theta_W)]^2\ . \quad (40b)$$

In (40) we have taken the hydrogen mass fraction of the Sun to be $X_{\rm H}=0.7$; we will use $n_{\rm He}/n_{\rm H}=0.1$ and follow Cameron[10] for the abundances of the other nuclei (we include H, He, C, N, O, Ne, Na, Mg, Al, Si, S, Ar, Ca, Cr, Fe, and Ni). Γ_{ν_D} is given in Table I.

It is of interest to compare the flux of neutrinos from

TABLE I. Parameters for Dirac neutrinos captured by the Sun.

m_{ν_D} (GeV)	Γ_{ν_D}	$R_{\nu_e}=R_{\nu_\mu}$	R_{ν_τ}	$R_{\rm tot}$	$\phi_\odot/\phi_\oplus$
1	3.1	2×10^{-16}	0	4×10^{-16}	
2	5.8	3×10^{-6}	0	6×10^{-6}	
3	7.8	2.9	0	5.8	2.5×10^3
4	9.3	3.7	0.07	7.5	1.3×10^3
8	14	5.3	0.82	12	2.9×10^2
12	18	6.8	1.8	15	1.3×10^2
16	22	7.2	2.6	17	76
20	25	4.7	2.0	11	53
24	28	3.0	1.4	7.4	41
28	31	1.9	1.0	4.8	33
32	34	1.1	0.6	2.8	29
36	37	0.6	0.3	1.5	27
40	39	0.2	0.1	0.5	23
48	44	0.015	0.01	0.04	20
60	50	0.75	0.55	2.0	19
70	54	2.1	1.6	5.7	19
80	58	4.0	3.1	11	19
90	61	6.4	5.1	18	19
100	64	9.3	7.6	26	20

annihilations in the Sun with those from annihilations in the Earth.[3] From Eqs. (20), (38), and (40) we may compute $\phi_\odot/\phi_\oplus$; our results are in Table I where we see that $\phi_\oplus \ll \phi_\odot$ for *all* m_{ν_D}. Note that we have ignored evaporation here; for $m_{\nu_D} \lesssim 6-10$ GeV, the flux from the Earth is much smaller than we have assumed.

Using the above cross section we may calculate the capture rate by the Sun of Dirac neutrinos and, from $\dot{N}_\odot$ and $\langle \sigma_a v \rangle_\odot$ compute $t_{\rm eq}$, $t_{\rm evap}$, and $N/N_{\rm eq}$. In Table II we show $t_{\rm eq}$, $\epsilon = t_{\rm eq}/2t_{\rm evap}$, and $N/N_{\rm eq}$ as a function of m_{ν_D}; note that $(N/N_{\rm eq})^2 \approx \frac{1}{2}$ for $m_{\nu_D} \approx 2.8$ GeV.

For the annihilation cross section given in (37) we may compute the various branching rations B_{Xf} as a function of the Dirac neutrino mass. Direct neutrino production is significant. $B_{\nu_D \nu}$ varies from 0.25 for $m_{\nu_D} = 3$ GeV to ~ 0.21 at higher masses; $\nu = \nu_e + \nu_\mu + \nu_\tau$. Over the same range $B_{\nu_D b}$ increases (from zero) to ~ 0.15. In contrast $B_{\nu_D c} \approx 0.12$ and $B_{\nu_D \tau} \approx 0.034$ are insensitive to m_{ν_D}. For further details see Tilav.[18]

With these results we may now compute the event rates for e, μ, and τ neutrinos ($R_{\nu_e} = R_{\nu_\mu}$); the results of our calculations are shown in Table I and Fig. 2. The falloff in R at low m_{ν_D} is due to evaporation. For $m_{\nu_D} \gtrsim 15$ GeV, R decreases due to the small abundance of such Dirac neutrinos in the Galaxy ($\bar{\rho}_X \propto \Omega_X < \Omega_N$); the dip in R is a reflection of the decrease in Ω_{ν_D} due to the resonant form of the annihilation cross section. For $m_{\nu_D} \lesssim 38$ GeV and $m_{\nu_D} \gtrsim 56$ GeV, R exceeds 1 event per kiloton year.

B. Majorana neutrinos

Since Majorana neutrinos are self-conjugate, the overall wave function must be antisymmetric so that s-wave annihilation is suppressed at low energies. The annihilation cross section is[19]

$$\sigma_a v = \frac{2G_F'^2}{\pi} \sum_f (1 - m_f^2/m_{\nu_M}^2)^{1/2} \left[(C_{Vf}^2 + C_{Af}^2) \frac{m_{\nu_M}^2 v^2}{6} + \frac{C_{Af}^2 m_f^2}{2} + (C_{Af}^2 - \tfrac{17}{4} C_{Vf}^2) \frac{m_f^2 v^2}{12} \right], \tag{41}$$

where G_F' is given in Eq. (36). This cross section should be divided by 2 to account for the identical nature of the annihilating particles. For annihilation in the early Universe $\langle v^2 \rangle_* = 6T_*/m_{\nu_M} = 6/x_*$ and

$$\langle \sigma_a v \rangle_* = \langle \sigma_a v \rangle_0 (a + b x_*^{-1}), \tag{42a}$$

where

$$\langle \sigma_a v \rangle_0 = \frac{G_F'^2 m_{\nu_M}^2}{2\pi} = 2.5 \times 10^{-28} \left[\frac{G_F'}{G_F} \right]^2 m_{\nu_M}^2 \ (\text{cm}^2 \text{sec}^{-1}), \tag{42b}$$

and

$$a = \sum_f (1 - m_f^2/m_{\nu_M}^2)^{1/2} C_{Af}^2 (m_f/m_{\nu_M})^2, \tag{42c}$$

$$b = \sum_f (1 - m_f^2/m_{\nu_M}^2)^{1/2} \times [2(C_{Vf}^2 + C_{Af}^2) + (C_{Vf}^2 - 17 C_{Af}^2/4)(m_f/m_{\nu_M})^2]. \tag{42d}$$

In computing the surviving abundance of relic Majorana neutrinos care must be taken since $\nu_M = \bar{\nu}_M$ so that $\rho_{\nu_M} = m_{\nu_M} n_{\nu_M}$:

TABLE II. Parameters relating to the evaporation of Dirac neutrinos from the Sun.

m_{ν_D} (GeV)	$t_{\rm eq}$ (Gyr)	ϵ	$N/N_{\rm eq}$
1.0	1.3	4.4×10^{7}	1.1×10^{-8}
1.5	0.64	2.9×10^{5}	1.7×10^{-6}
2.0	0.077	4.5×10^{2}	1.1×10^{-3}
2.5	0.045	3.7	0.13
2.6	0.042	1.5	0.31
2.7	0.039	0.59	0.57
2.8	0.036	0.24	0.79
2.9	0.034	0.095	0.91
3.0	0.032	0.039	0.96
3.1	0.030	0.016	0.98
3.2	0.028	0.0064	0.99
3.3	0.027	0.0026	1.0
3.4	0.025	0.0011	1.0
3.5	0.024	0.0004	1.0

$$\Omega_{\nu_M} h_{1/2}{}^2 = \frac{7.7}{m_{\nu_M}{}^2} \left[\frac{x_*}{g_*{}^{1/2}} \right] (a + b/2x_*)^{-1} \left[\frac{G_F'}{G_F} \right]^{-2} . \tag{43}$$

In Fig. 3, $\Omega_{\nu_M} h_{1/2}{}^2$ is shown as a function of m_{ν_M}. For relatively small m_{ν_M}, $\Omega_{\nu_M} h_{1/2}{}^2 = 1$ (0.04) for $m_{\nu_M} = 5$ (27) GeV. For much larger values of m_{ν_M}, $\Omega_{\nu_M} h_{1/2}{}^2$ increases to 0.04 at $m_{\nu_M} = 78$ GeV.

For "cold" annihilation in the Sun we may neglect the terms proportional to v^2 (s-wave annihilation dominates) so that

$$\langle \sigma_a v \rangle_\odot = \langle \sigma_a v \rangle_0 a = 2.5 \times 10^{-28} (G_F'/G_F)^2 \times \sum_f (1 - m_f{}^2/m_{\nu_M}{}^2)^{1/2} C_{Af}{}^2 m_f{}^2 (\mathrm{cm}^3 \mathrm{sec}^{-1}) . \tag{44}$$

Because of the $m_f{}^2$ dependence, annihilations of Majorana neutrinos directly to ordinary neutrinos are suppressed. However, the same mass dependence ensures a sizable branching ratio for annihilations to heavy fermions (b,c,τ). For $m_{\nu_M} \gtrsim 10$ GeV, $B_{\nu_M c} \sim 0.1$, $B_{\nu_M \tau} \approx 0.05$, and $B_{\nu_M b} \approx 0.84$. For further details see Tilav.[18]

Majorana neutrinos scatter primarily from hydrogen nuclei in the Sun (since $\nu_M = \bar{\nu}_M$, $Y_L = -Y_R$, and $\bar{Y} = 0$) with a cross section given by (39):

$$\sigma_{\mathrm{eff}\odot} = X_{\mathrm{H}} \sigma_{\nu_M \mathrm{H}} = 1.5 \times 10^{-38} \left[\frac{m_{\nu_M}}{m_{\nu_M} + m_{\mathrm{H}}} \right]^2 \mathrm{cm}^2 . \tag{45}$$

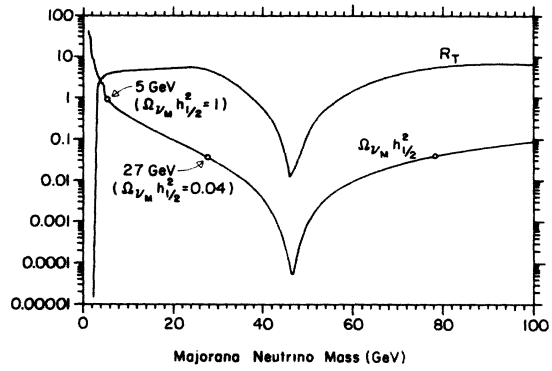

FIG. 3. The event rate (R_T) per kiloton year for neutrinos from the annihilation of heavy Majorana neutrinos captured by the Sun. Also shown is the relic density ($\Omega_{\nu_M} h_{1/2}{}^2$) of such Majorana neutrinos.

With the above cross section we may calculate $\dot{N}_\odot$, t_{eq}, t_{evap}, and N/N_{eq} for capture of Majorana neutrinos by the Sun. We display our results in Table III; note that $(N/N_{\mathrm{eq}})^2 \approx \frac{1}{2}$ for $m_{\nu_M} = 3.0$ GeV.

The event rates due to annihilations of Majorana neutrinos captured by the Sun are given in Table IV and Fig. 3. For $m_{\nu_M} \lesssim 38$ GeV and $m_{\nu_M} \gtrsim 57$ GeV, R_{tot} exceeds 1 event per kiloton year.

C. Scalar neutrinos

The lightest supersymmetric particle (LSP) may be stable and, if sufficiently massive, a candidate for cold-dark matter. The lightest scalar neutrino—the superpartner of the neutrinos ($\tilde{\nu}_e$,$\tilde{\nu}_\mu$,$\tilde{\nu}_\tau$)—is a candidate for the LSP.[20] Scalar-neutrino annihilation, however, is very sen-

TABLE III. Parameters relating to the evaporation of Majorana neutrinos from the Sun.

m_{ν_M} (GeV)	t_{eq} (Gyr)	ϵ	N/N_{eq}
1.0	2.75	8.5×10^{7}	5.9×10^{-9}
1.5	2.05	8.0×10^{5}	6.1×10^{-7}
2.0	0.34	1.6×10^{3}	3.0×10^{-4}
2.5	0.25	16	3.1×10^{-2}
2.6	0.24	6.5	7.6×10^{-2}
2.7	0.24	2.7	0.18
2.8	0.23	1.1	0.39
2.9	0.22	0.45	0.65
3.0	0.22	0.19	0.83
3.1	0.21	0.08	0.93
3.2	0.20	3.2×10^{-2}	0.97
3.3	0.20	1.3×10^{-2}	0.98
3.4	0.20	5.5×10^{-3}	0.99
3.5	0.20	2.3×10^{-3}	0.99
3.6	0.19	9.5×10^{-4}	0.99
3.7	0.19	4.0×10^{-4}	1.00
3.8	0.19	1.5×10^{-4}	1.00

TABLE IV. Event rates for Majorana neutrinos.

m_{ν_M} (GeV)	$R_{\nu_e}=R_{\nu_\mu}$	R_{ν_τ}	$R_{\rm tot}$
1			
2			
3	0.66		1.3
4	1.6	4×10^{-4}	3.1
8	2.1	0.073	4.3
12	2.3	0.22	4.8
16	2.4	0.35	5.1
20	2.4	0.49	5.4
24	2.5	0.60	5.6
28	2.2	0.6	5.0
32	1.2	0.4	2.8
36	0.6	0.2	1.4
40	0.23	0.08	0.54
48	0.015	0.006	0.036
60	0.6	0.3	1.5
70	1.6	0.8	4.0
80	2.6	1.4	6.6
90	2.6	1.4	6.6
100	2.6	1.5	6.7

sitive to the mixing parameters of the neutral sector of supersymmetry.[20] Since scalar neutrinos may annihilate via gauge/Higgs fermion exchange, $\langle\sigma_a v\rangle$ is usually very large[20] and, correspondingly, $\Omega_{\tilde\nu}$ is very small [see Eq. (9)].

Ibanez[20] has called attention to the possibility that scalar-neutrino annihilation could be dominated by the exchange of the Majorana part of the Z gaugino ($\tilde Z$). For this case, the annihilation cross section is independent of the $\tilde\nu$ mass and may be large or small depending on the arbitrary value of $M_{\tilde Z}$—the Majorana part of the Z-gaugino mass:[20]

$$\sigma_a v\approx\frac{G_F^{\,2}}{\pi}M_{\tilde Z}^{\,2}\approx5.0\times10^{-28}M_{\tilde Z}^{\,2}\ \text{cm}^3\text{sec}^{-1}\ . \tag{46}$$

For $M_{\tilde Z}\approx M_{Z^0}$, $\sigma_a v$ is very large and, therefore, $\Omega_{\tilde\nu}$ is very small; in this limit, scalar neutrinos are not cold-dark-matter candidates ($\Omega_{\tilde\nu}\ll\Omega_N$). If, however, $M_{\tilde Z}$ is sufficiently small ($M_{\tilde Z}\lesssim30$ GeV), $\Omega_{\tilde\nu}\gtrsim\Omega_N$ [see Eq. (9)] and scalar neutrinos may be cosmologically interesting. The bottom line, however, is that any conclusions we might draw regarding scalar neutrinos are likely to be strongly model dependent. With this caution in mind, we will *assume*[20] that $\Omega_{\tilde\nu}h_{1/2}^{\,2}\approx1$ (or, $\Omega_{\tilde\nu}>\Omega_N$) and proceed to discuss the consequences of capture by the Sun.

Scalar neutrinos scatter from nuclei through Z^0 exchange with coherent vector as well as axial-vector couplings. The $\tilde\nu$-nucleus elastic scattering cross sections are given by Eqs. (38) and (39) with the exception that the hypercharge of the scalar neutrino is $\overline{Y}_{\tilde\nu}=-1$. In analogy with Eqs. (40),

$$\sigma_{\text{eff}\odot}=0.7\frac{G_F^{\,2}}{8\pi}(4)\Gamma_{\tilde\nu}\approx5.8\times10^{-39}\Gamma_{\tilde\nu}\ \text{cm}^2\ , \tag{47a}$$

where

$$\Gamma_{\tilde\nu}=\Gamma_{\nu_D}-12\left[\frac{m_{\rm H}m_{\tilde\nu}}{m_{\rm H}+m_{\tilde\nu}}\right]^2[(2\sin^2\theta_W-\tfrac{1}{2})^2+\tfrac{3}{4}]\ . \tag{47b}$$

The Sun captures scalar neutrinos at a rate

$$\dot N_\odot=5.1\times10^{26}(\Gamma_{\tilde\nu}/m_{\tilde\nu})(\bar\rho_{\tilde\nu}/\bar v_{\tilde\nu})\ \text{sec}^{-1}\ . \tag{48}$$

The calculation of $t_{\rm eq}$ and, hence, ϵ for scalar neutrinos is uncertain due to the extreme model dependence of the annihilation cross section. If we assume an annihilation cross section such that $\Omega_{\tilde\nu}h_{1/2}^{\,2}\approx1$, we find[18] that $(N/N_{\rm eq})^2\approx\frac{1}{2}$ for $m_{\tilde\nu}=2.8$ GeV.

TABLE V. Event rates for scalar neutrinos.

$m_{\tilde\nu}$ (GeV)	$R_{\nu_e}=R_{\nu_\mu}$	R_{ν_τ}
1		
2	0.013	
3	54	
4	71	1.6
8	130	24
12	190	60
16	250	100
20	310	150
24	360	190
28	410	230
32	460	280
36	500	330
40	540	370
50	640	470
60	730	570
70	800	640
80	870	710
90	920	780
100	970	830

If the dominant product of the annihilation of scalar neutrinos of type i is ordinary neutrinos of type i ($\tilde{\nu}_i\tilde{\nu}_i \to \nu_i\nu_i$) so that $B_{\tilde{\nu}\nu}=1$, the event rate from monoenergetic neutrinos produced by annihilations in the Sun will be

$$R_{\nu_e}(R_{\nu_\mu}) = 17.3\Gamma_{\tilde{\nu}}(N/N_{\rm eq})^2(\bar{\rho}_{\tilde{\nu}}/\bar{v}_{\tilde{\nu}})\ ({\rm kt\,yr})^{-1}\ , \quad (49a)$$

or

$$R_{\nu_\tau} = 17.3\Gamma_{\tilde{\nu}}(N/N_{\rm eq})^2(\bar{\rho}_{\tilde{\nu}}/\bar{v}_{\tilde{\nu}})\langle y(m_{\tilde{\nu}})\rangle\ ({\rm kt\,yr})^{-1}\ . \quad (49b)$$

Our results (assuming $\Omega_{\tilde{\nu}}h_{1/2}{}^2=1$) are shown in Table V. It is clear that if the e or μ scalar neutrino is the LSP, significant event rates are expected for $m_{\tilde{\nu}} \gtrsim 3$ GeV; if the τ scalar neutrino is the LSP, significant event rates are expected for $m_{\tilde{\nu}} \gtrsim 4$ GeV. As with Dirac neutrinos, capture by the Sun dominates the Earth for the predicted event rate.

D. Photinos

Photinos annihilate through the exchange of scalar fermions.[7,21] In general, the masses of the various scalar fermions need not be identical and, therefore, the photino annihilation cross section may depend on many adjustable parameters. In many models, however, it is the case that the scalar-fermion masses are degenerate ($\equiv m_S$) and, therefore, the photino annihilation cross section simplifies considerably:[21]

$$\sigma_a v = \frac{1}{2\pi}\left[\frac{m_{\tilde{\gamma}}}{m_S{}^2+m_{\tilde{\gamma}}{}^2}\right]^2 \sum_f Q_F{}^4(1-m_f{}^2/m_{\tilde{\gamma}}{}^2)^{1/2}\left\{\left[\frac{m_f}{m_{\tilde{\gamma}}}\right]^2+\left[1-\left[\frac{m_f}{m_{\tilde{\gamma}}}\right]^2\right]\frac{v^2}{3}\right\}. \quad (50)$$

In (50), Q_f (m_f) are the charge (mass) of the fermion in $\tilde{\gamma}\tilde{\gamma}\to f\bar{f}$. $Q_f \equiv q_f\sqrt{4\pi\alpha}$, where α is the fine-structure constant and q_f is the charge in units of the electron charge. As with Majorana neutrinos, photinos—which are Majorana particles—have suppressed s-wave annihilation at low energy. In the early Universe,

$$\langle\sigma_a v\rangle_* = \langle\sigma_a v\rangle_0(a+bx_*{}^{-1})\ , \quad (51a)$$

where

$$\langle\sigma_a v\rangle_0 = 7.8\times10^{-29}(100/m_S)^4 \times[1+(m_{\tilde{\gamma}}/m_S)^2]^{-2}m_{\tilde{\gamma}}{}^2\ {\rm cm^3 sec^{-1}}\ , \quad (51b)$$

$$a = \sum_f q_f{}^4[1-(m_f/m_{\tilde{\gamma}})^2]^{1/2}(m_f/m_{\tilde{\gamma}})^2\ , \quad (51c)$$

$$b = 2\sum_f q_f{}^4[1-(m_f/m_{\tilde{\gamma}})^2]^{3/2}\ . \quad (51d)$$

In contrast with the particle candidates discussed heretofor, the survival of relic photinos depends on (at least) two parameters, $m_{\tilde{\gamma}}$ and m_S:

$$\Omega_{\tilde{\gamma}}h_{1/2}{}^2 = 24.6\left[\frac{x_*}{g_*{}^{1/2}}\right]\left[a+\frac{b}{2x_*}\right]^{-1} \times\left[\frac{1}{m_{\tilde{\gamma}}{}^2}\right]\left[\frac{m_S}{100}\right]^4\left[1+\left[\frac{m_{\tilde{\gamma}}}{m_S}\right]^2\right]^2. \quad (52)$$

Figure 4 shows the $m_{\tilde{\gamma}}$ vs m_S relation for $\Omega_{\tilde{\gamma}}h_{1/2}{}^2=1$. For stable photinos the shaded region to the right and below this curve is excluded. The dashed curve shows the locus of $m_{\tilde{\gamma}}, m_S$ values for which $\Omega_{\tilde{\gamma}}h_{1/2}{}^2=0.04$. In the region to the left of this curve, photinos would be dynamically unimportant ($\Omega_{\tilde{\gamma}} < \Omega_N$). We also show the $m_{\tilde{\gamma}}=m_S$ line in Fig. 4. The region above this line is excluded if the photino is the lightest supersymmetric particle. Note that if the photino is the LSP and if $m_{\tilde{\gamma}}$ exceeds $\sim$50 GeV, photinos *are* dynamically important ($\Omega_{\tilde{\gamma}} > \Omega_N; \Omega_{\tilde{\gamma}}h_{1/2}{}^2 > 0.04$).

For "cold" annihilation in the Sun ($v^2\to 0$), $\langle\sigma_a v\rangle_\odot = \langle\sigma_a v\rangle_0 a$; from the dependence of a on the charges and masses of the final-state fermions we may determine the various branching ratios. Annihilation to ordinary neutrinos is absent and, for $m_{\tilde{\gamma}} \gtrsim 8$ GeV, $B_{\tilde{\gamma}\tau}\approx 0.60$, $B_{\tilde{\gamma}c}\approx 0.24$, $B_{\tilde{\gamma}b}\approx 0.13$; for details see Ref. 18.

Photinos scatter in the Sun mainly from hydrogen with a cross section[17] dominated by scalar—up-quark exchange. For $m_S \gg m_{\tilde{\gamma}}$,

$$\sigma_{\tilde{\gamma}{\rm H}} = 0.91\left[\frac{4}{\pi}\right]\left[\frac{2}{3}\right]^4\frac{m_{\tilde{\gamma}}{}^2}{m_S{}^4}\left[\frac{m_{\rm H}}{m_{\rm H}+m_{\tilde{\gamma}}}\right]^2. \quad (53)$$

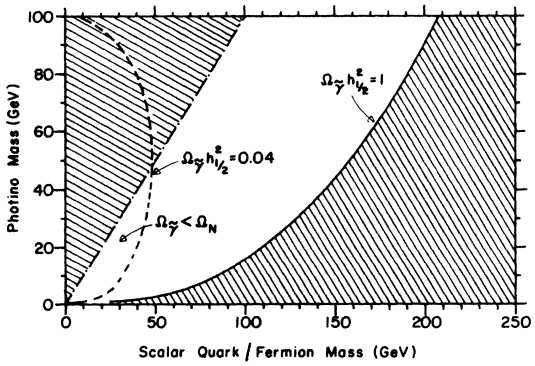

FIG. 4. Curves for the relic density of photinos ($\Omega_{\tilde{\gamma}}h_{1/2}{}^2$) are shown in the photino-mass ($m_{\tilde{\gamma}}$)—scalar-fermion-mass (m_S) plane. Stable photinos in the right-hand shaded region would contribute in excess of the critical density. Photinos above the $m_{\tilde{\gamma}}=m_S$ line would not be the LSP.

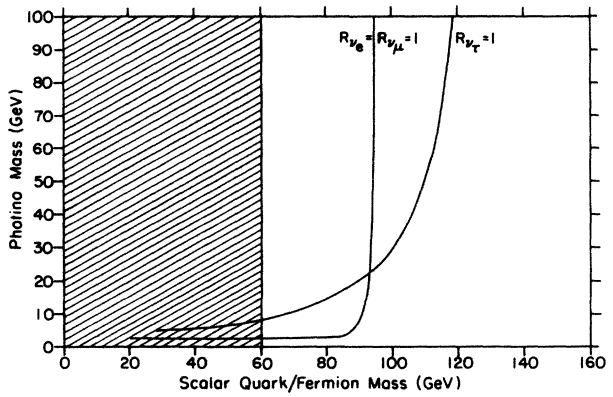

FIG. 5. Curves for an event rate of one event per kiloton year for $e(\mu)$ neutrinos and for τ neutrinos from the annihilation of photinos captured by the Sun are shown in the $m_{\tilde{\gamma}}$-m_S plane. The regions to the left of the curves correspond to $R>1$. The shaded region ($m_S \lesssim 60$ GeV) is excluded (Ref. 22) by data from accelerator experiments.

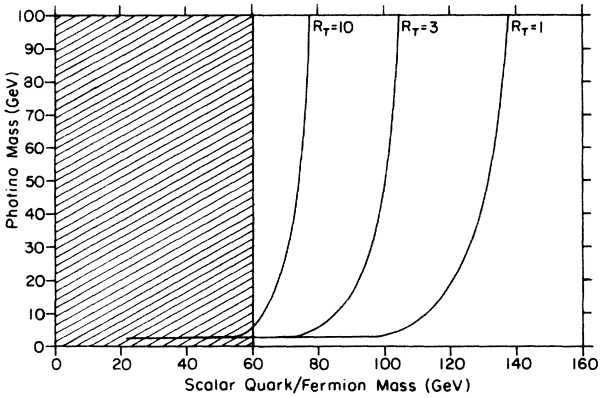

FIG. 6. Curves for 1, 3, and 10 events per kiloton year for all neutrinos from the annihilation of photinos captured by the Sun are shown in the $m_{\tilde{\gamma}}$-m_S plane. The shaded region is excluded (Ref. 22) by accelerator data.

The photino capture rate in the Sun is

$$\dot{N}_\odot = \frac{4\times 10^{26}}{m_{\tilde{\gamma}}}\left[\frac{m_{\tilde{\gamma}}}{m_{\tilde{\gamma}}+m_H}\right]^2\left[\frac{100}{m_S}\right]^4\left[\frac{\bar{\rho}_{\tilde{\gamma}}}{\bar{v}_{\tilde{\gamma}}}\right]\ \text{sec}^{-1}\ . \quad (54)$$

In computing the time scale t_{eq} for a steady-state abundance of photinos to be accreted by the Sun, the product $\dot{N}_\odot\langle\sigma_a v\rangle_\odot$ enters [see Eq. (18)]. Comparing (18), (51), and (54) we see that t_{eq} is proportional to $m_S{}^4$ for $m_S \gg m_{\tilde{\gamma}}$. However, since t_{evap} varies as $\sigma_{eff\odot}{}^{-1}$ [see Eq. (21)] and $\sigma_{eff\odot}\propto m_S{}^{-4}$, the ratios ϵ and N/N_{eq} are *independent* of m_S. In Table VI we give $t_{eq}(100/m_S)^4$, ϵ, and N/N_{eq} as a function of $m_{\tilde{\gamma}}$; note that $m_{\tilde{\gamma},evap}\approx 2.9$ GeV.

In general, the neutrino-induced event rates due to photino annihilation in the Sun depend on *both* $m_{\tilde{\gamma}}$ and m_S. In Fig. 5 we show curves in the $m_{\tilde{\gamma}}$,m_S plane for R_{ν_e} $(=R_{\nu_\mu})=1$ event per kiloton year and $R_{\nu_\tau}=1$ event per kiloton year and, in Fig. 6 we show curves for $R_{tot}=1$, 3, 10 events per kiloton year. Notice that our curves for the event rate "end" at minimum values of $m_{\tilde{\gamma}}$ and m_S. The reason is that when $\Omega_{\tilde{\gamma}}<\Omega_N$, $\rho_{\tilde{\gamma}}\propto\Omega_{\tilde{\gamma}}\propto m_S{}^4$ so that R is then (for smaller values of m_S) independent of m_S. In principle then the predicted event rate would not yield any bound to $m_{\tilde{\gamma}}$ for $m_S<m_{S,min}$. However, from an analysis of the UA1 data, Barnett, Haber, and Kane[22] have derived a *lower* bound to m_S: $m_S\gtrsim 60$ GeV; this bound is also shown in Figs. 5 and 6.

If, instead of fixing R, we set $\Omega_{\tilde{\gamma}}h_{1/2}{}^2=1$, we may compute m_S, R_{ν_e} $(=R_{\nu_\mu})$, and R_{ν_τ} as a function of $m_{\tilde{\gamma}}$. The results are given in Table VII.

IX. DISCUSSION AND CONCLUSIONS

For each of the ("cold-") dark-matter candidates considered (ν_D, ν_M, $\tilde{\nu}$, $\tilde{\gamma}$) we have calculated the contributions to the universal mass density ($\Omega_X h_{1/2}{}^2$) and, the contribution to the neutrino-induced event rate in underground

TABLE VI. Parameters relating to the evaporation of photinos from the Sun.

$m_{\tilde{\gamma}}$ (GeV)	$t_{eq}(100/m_S)^4$ (Gyr)	ϵ	N/N_{eq}
1.0	4.5	4×10^{7}	1×10^{-8}
1.5	3.4	4×10^{5}	1×10^{-6}
2.0	0.55	8×10^{2}	6×10^{-4}
2.5	0.41	7.8	0.064
2.6	0.39	3.2	0.15
2.7	0.38	1.3	0.34
2.8	0.37	0.53	0.60
2.9	0.36	0.22	0.80
3.0	0.35	0.091	0.91
3.1	0.34	0.038	0.96
3.2	0.34	0.016	0.99
3.3	0.33	0.0064	0.99
3.4	0.32	0.0027	1.0
3.5	0.32	0.0011	1.0
3.6	0.31	0.0005	1.0

TABLE VII. Event rates for photinos with $\Omega_{\tilde{\gamma}} h_{1/2}{}^2 = 1$.

$m_{\tilde{\gamma}}$	m_S (GeV)	$R_{\nu_e} = R_{\nu_\mu}$	R_{ν_τ}	$R_{\rm tot}$
1	24			
2	45			
3	55	5.3		11
4	62	4.1		8.3
8	76	2.0	0.30	4.4
12	88	1.2	0.46	2.8
16	99	0.72	0.47	1.9
20	108	0.49	0.43	1.4
24	116	0.36	0.38	1.1
28	124	0.27	0.34	0.88
32	131	0.27	0.28	0.70
36	138	0.17	0.25	0.59
40	144	0.14	0.22	0.50
50	158	0.09	0.17	0.35
60	170	0.06	0.13	0.25
70	180	0.05	0.11	0.21
80	190	0.04	0.09	0.17
90	199	0.03	0.07	0.13
100	207	0.02	0.06	0.10

detectors following capture by the Sun and subsequent annihilation. A constraint on the masses of the candidate WIMP's follows from the requirement that the present density not be too large: $\Omega_X h_{1/2}{}^2 \lesssim 1$; particles whose masses are such that this constraint is violated must be unstable.

For Dirac neutrinos, the density constraint requires that $m_{\nu_D} \gtrsim 3.6$ GeV; for $m_{\nu_D} \gtrsim 15$ GeV, Dirac neutrinos are dynamically less important than nucleons ($\Omega_{\nu_D} \lesssim \Omega_N$). Dirac neutrinos with masses in the ranges $\lesssim 38$ GeV and $\gtrsim 56$ GeV, yield a significant rate from annihilation produced energetic neutrinos (see Table I and Fig. 2). Such an event rate should be (have been) detectable. Implicit in our analysis, however, has been the assumption of particle-antiparticle symmetry ($N_X = N_{\bar{X}}$). For photinos and Majorana neutrinos which are their own antiparticles, this assumption plays no role. Furthermore, since scalar neutrinos annihilate with themselves ($\tilde{\nu}_i \tilde{\nu}_i \to \nu_i \nu_i$), asymmetry would not change our results there either. However, for Dirac neutrinos, the assumption of symmetry is crucial. For degenerate Dirac neutrinos ($N_{\bar{\nu}_D} \ll N_{\nu_D}$ or, vice versa) annihilation can be suppressed; this possibility is being investigated by [D. Seckel (private communication)].

For Majorana neutrinos, $\Omega_{\nu_M} h_{1/2}{}^2 \lesssim 1$ for $m_{\nu_M} \gtrsim 5$ GeV and $\Omega_{\nu_M} \lesssim \Omega_N$ for $27 \lesssim m_{\nu_M} \lesssim 78$ GeV. For masses in the range $\lesssim 38$ GeV and $\gtrsim 57$ GeV, the expected event rate due to annihilation neutrinos (see Table IV and Fig. 3) exceeds 1 per kiloton year. As with Dirac neutrinos, massive Majorana neutrinos, if they are the halo dark mass, yield, through their capture by the Sun, a detectable event rate.

It must, however, be emphasized here that such massive (Dirac *or* Majorana) neutrinos are not expected to be stable on a cosmological time scale ($t_0 \approx 10$–20 Gyr ≈ 3–6×10^{17} sec). For example, a heavy neutrino could decay via $\nu_X \to l\pi$ very rapidly[23]

$$\tau_X \approx 2 \times 10^{-10} m_{Xl}{}^{-3} \, | \, U_{Xl} \, | \, {}^{-2} \ (\text{sec}) \ , \tag{55}$$

provided that the ν_X-lepton (e,μ,τ) mixing is not incredibly small (for $\tau_X \gtrsim t_0$, $| \, U_{Xl} \, | < 2.5 \times 10^{-14} m_X{}^{-3/2}$). It is very unlikely, then, that massive Dirac or Majorana neutrinos are viable cold-dark-matter candidates.

Scalar neutrinos are problematic as cold-dark-matter candidates. In many models, the scalar neutrino annihilation cross section is very large and this results in very few $\tilde{\nu}$ surviving the early Universe ($\Omega_{\tilde{\nu}}$ is "usually" very small: $\Omega_{\tilde{\nu}} \ll \Omega_N$). In some—not very "natural"—models it may be possible to tune the annihilation cross section so that $\Omega_{\tilde{\nu}} h_{1/2}{}^2 = 1$ (Refs. 20 and 21). If, indeed, $\tilde{\nu}$ are the dark mass of the halo, the expected event rate from capture by the Sun followed by annihilation ($\tilde{\nu}\tilde{\nu} \to \nu\nu$) is enormous (see Table V) for $m_{\tilde{\nu}} \gtrsim 3$ GeV (if the LSP is $\tilde{\nu}_e$ or $\tilde{\nu}_\mu$) or for $m_{\tilde{\nu}} \gtrsim 8$ GeV (if the LSP is $\tilde{\nu}_\tau$).

Of the WIMP's we have considered, photinos remain as possibly viable cold-dark-matter candidates. For photinos there are (at least) two adjustable parameters: the photino mass $m_{\tilde{\gamma}}$ and the scalar-fermion mass m_S. Dynamically interesting photinos are restricted to have $m_{\tilde{\gamma}}$, m_S in the area shown in Fig. 4. Photinos with $m_{\tilde{\gamma}} \gtrsim 2.9$ GeV (see Table VI) will be captured and retained by the Sun long enough to accumulate in the core and annihilate. In Fig. 6 is shown the locus of $m_{\tilde{\gamma}}, m_S$ corresponding to several (total) event rates due to annihilation neutrinos. Event rates in excess of those indicated on the curves are found to the left and above the curves. Also shown in Figs. 5 and 6 is the line corresponding to the accelerator limit[22] to m_S; $m_S \lesssim 60$ GeV is excluded by the UA1 data.[22] Note that if we impose the constraint that m_S exceed ~ 60 GeV, photinos—if they are the LSP—are always dynami-

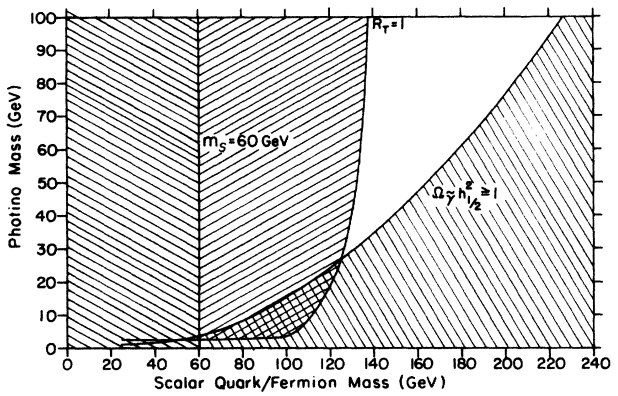

FIG. 7. For photinos, the excluded (shaded) regions of the $m_{\tilde\gamma}$-m_S plane—assuming $R_T>1$ is detectable—are shown (see the text).

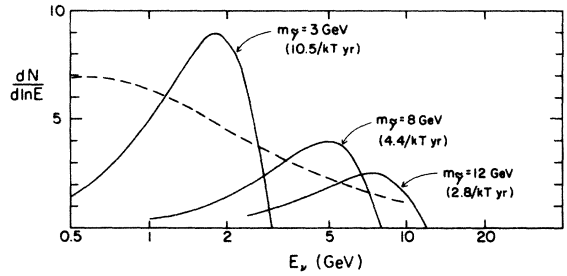

FIG. 8. The differential neutrino-induced event rate (for all neutrino flavors) from the annihilation of photinos captured by the Sun for $m_{\tilde\gamma}=3,8,12$ GeV; in each case m_S has been chosen so that $\Omega_{\tilde\gamma}h_{1/2}{}^2=1$ (see Table VII). Dashed line shows the background due to atmospheric neutrinos within a cone of half-angle 37°.

cally important; for $m_S\gtrsim 60$ GeV, $\Omega_{\tilde\gamma}h_{1/2}{}^2\gtrsim 0.06$.

As an illustrative example, in Fig. 7 we show in the $m_{\tilde\gamma}$-m_S plane the curves for $\Omega_{\tilde\gamma}h_{1/2}{}^2=1$, $R_{\rm tot}=1$, and $m_S=60$ GeV. The shaded region to the right and below the curve $\Omega_{\tilde\gamma}h_{1/2}{}^2=1$ is excluded by the density constraint. Accelerator data[22] excludes the region $m_S\lesssim 60$ GeV. If it should prove possible to reach a level of ~ 1 event per kiloton year in the underground detectors, photinos with $m_{\tilde\gamma}$,m_S in the area to the left and above the curve labeled $R_{\rm tot}=1$ would be detectable or excludable. Since a variety of $m_{\tilde\gamma}$,m_S combinations may allow photinos to be the cold-dark matter of the halo of the Galaxy, it is desirable to study the expected event rate from $\tilde\gamma$ captures in the Sun in more detail.

It should first be emphasized that the energetic neutrinos from $\tilde\gamma$ annihilation in the Sun carry directional information. For the charged-current interaction of $\gtrsim$ GeV νs an angular resolution of $\lesssim 37°$ is reasonable (the higher the ν energy, the better the resolution), the atmospheric background, to which the $\tilde\gamma$-annihilation signal should be compared, is reduced by a factor of $\gtrsim 10$.

Spectral information can be employed to further distinguish atmospheric background neutrinos from annihilation-produced neutrinos. The differential event rate (per unit energy interval) for the background signal is concentrated at low energy in contrast with that from the annihilation of relatively massive photinos (recall that $\langle E_\nu\rangle\approx\frac{1}{3}m_{\tilde\gamma}$). To illustrate this effect we have, in Fig. 8, compared the differential event rates from atmospheric background neutrinos (divided by 10 to account for those within $\theta<37°$) with those predicted for several values of the photino mass with m_S adjusted so that $\Omega_{\tilde\gamma}h_{1/2}{}^2=1$. We note that even though the total event rate from $\tilde\gamma$ annihilation decreases with increasing $m_{\tilde\gamma}$ (for $\Omega_{\tilde\gamma}h_{1/2}{}^2=1$, see Table VII), even relatively high-mass photinos will produce neutrinos which should be distinguishable above background.

We have, so far, computed the event rate due to neutrinos which interact in the detector. However, μ neutrinos of sufficiently high energy can interact in the rock surrounding the detector and produce muons which pass through the detector and are recorded. At sufficiently high neutrino energies this signal becomes comparable to (and eventually exceeds) the signal from interactions inside the detector volume.

The external signal can be written as[24]

$$\frac{dS}{dE_\nu}=\phi_\nu(E_\nu)P_{\nu\to\mu}(E_\nu)+\phi_{\bar\nu}(E_\nu)P_{\bar\nu\to\mu}(E_{\bar\nu})\ , \tag{56}$$

where $\phi_\nu=\phi_{\bar\nu}$ is the neutrino flux from Eq. (1) and $P_\nu(P_{\bar\nu})$ is the probability that a neutrino (antineutrino) of energy E_ν aimed at the detector sends a muon into the detector with energy above threshold ($E_{\mu 0}$) for detection. P_ν is essentially the neutrino cross section times the number of target nucleons per unit area within muon range of the detector. Since both σ_ν and muon range increase linearly with energy, P_ν is proportional to $E_\nu{}^2$ until the range and cross section cutoff at high energy. Neglecting the contribution of antiquarks to $\nu_\mu+N\to\mu+$anything, a simple approximation for P_ν is[25]

$$P(E_\nu)\equiv P_\nu+P_{\bar\nu}\simeq\frac{N_A\sigma_0}{\alpha}\frac{(E_\nu-E_{\mu 0})^2}{2}\left[\frac{3}{2}+\frac{1}{3}\left[\frac{E_{\mu 0}}{E_\nu}\right]+\frac{1}{6}\left[\frac{E_{\mu 0}}{E_\nu}\right]^2\right]\ , \tag{57}$$

where $\sigma_0\simeq 0.7\times 10^{-38}$ cm^{2}GeV^{-1} and $\alpha\simeq 0.002$ GeV cm^2/g is the energy-loss rate of muons due to ionization. Equation (57) is valid for $E_\mu\leq E_\nu\ll 500$ GeV where ionization is the dominant energy-loss mechanism for muons. The rate of contained vertices per year [see Eqs. (1)—(6)] is

$$R_i V_{kt}=190(\tfrac{1}{2}\dot N_X)\frac{m_X}{4\pi R^2}\sum_f B_{Xf}B_{fi}\langle y\rangle_{fi}V_{kt}\ . \tag{58}$$

In contrast the external ν_μ-induced rate is

$$R_\mu(\text{external}) = 600(\tfrac{1}{2}\dot{N}_X)\frac{m_X{}^2}{4\pi R^2}\sum_f B_{Xf}B_{f\nu_\mu}A_{1000}FI_{f\nu_\mu}\ , \tag{59}$$

where A_{1000} is the projected area of the detector normal to the muon trajectory (in units of 1000 m^2) and

$$I_{f\nu_\mu} = \int_{y_0}^{1}\frac{(y-y_0)^2}{2}\left[\frac{3}{2}+\frac{1}{3}\left[\frac{y_0}{y}\right]+\frac{1}{6}\left[\frac{y_0}{y}\right]^2\right]g_{f\nu_\mu}(y)dy\ . \tag{60}$$

In Eq. (59) F is the fraction of time the Sun is below the horizon (only upward muons can be identified as ν induced because of the huge background of downward atmospheric cosmic-ray muons). Then, for $E_\nu \ll 500$ GeV, the ratio of external to internal signal is

$$\frac{R_\mu(\text{external})}{V_{kt}\sum_i R_i(\text{contained})} \equiv \frac{3.2A_{1000}m_X}{V_{kt}}\left[\frac{\sum_f B_{Xf}B_{f\nu_\mu}}{\sum_i\sum_f B_{Xf}B_{fi}}\right]\frac{I}{\langle y\rangle}F\ . \tag{61}$$

To evaluate I we transform Eqs. (26) and (27) into the laboratory frame and use the average of $g_{c\nu_\mu}$ and $g_{b\nu_\mu}=g_{\tau\nu_\mu}$, namely,

$$g(y) = \tfrac{11}{6} - \tfrac{9}{2}y^2 + \tfrac{8}{3}y^3\ . \tag{62}$$

$F \simeq \frac{1}{2}$ and the ratio of branching ratios in Eq. (61) is also $\simeq \frac{1}{2}$. Figure 9 displays the ratio of events of external origin to internal events for $A_{1000}/V_{kt}=0.12$, approximately the parameter of the Irvine-Michigan-Brookhaven (IMB) detector. External and internal rates for various $m_{\tilde{\gamma}}$ are compared in Table VIII assuming $A_{1000}=0.4$, $V_{kt}=3.3$ and $\Omega_{\tilde{\gamma}}h_{1/2}{}^2=1$. For high-mass photinos ($m_{\tilde{\gamma}} \gtrsim 20$ GeV), the external events dominate over the contained events and, therefore, may help to detect or exclude such high-mass WIMP's.

If, indeed, photinos were to account for the dark mass of the Galaxy halo, occasional $\tilde{\gamma}\tilde{\gamma}$ annihilation would occur in the interstellar medium. Among the products of such annihilation would be high-energy γ rays, positrons, and antiprotons.[26] For example, Silk and Srednicki[26] suggest that annihilation of photinos with $m_{\tilde{\gamma}} \approx 3$ GeV and $m_S \approx 50$ GeV may account for the observed,[27] low-energy flux of cosmic-ray antiprotons. In contrast, Stecker, Rudaz, and Walsh[26] suggest the same flux be accounted for by photinos with $m_{\tilde{\gamma}} \approx 15$–$20$ GeV and $m_S \approx 30$–25 GeV. Finally, Hagelin and Kane[26] have explored a variety of models (combinations of $m_{\tilde{\gamma}}$ and m_S) and find possible fits to the data with $m_{\tilde{\gamma}} \approx 3$–$7$ GeV and $m_S \approx 75$ GeV. The UA1 data would seem to exclude those cases with $m_S \lesssim 60$ GeV (Ref. 22). Even ignoring this constraint, the expected event rate from annihilation in the Sun provides a constraint on these models. In Table IX we evaluate $\Omega_{\tilde{\gamma}}h_{1/2}{}^2$ and, more to the point, R_{tot} for a variety of choices of $m_{\tilde{\gamma}}$ and m_S. The suggestion by Stecker, Rudaz, and Walsh[26] for the origin of the cosmic ray flux of antiprotons is clearly excluded. Depending on the actual sensitivity of the underground detectors, the other suggested[26] possibilities can most likely be excluded too. It must, however, be noted that for $m_{\tilde{\gamma}} \lesssim 2.9$ GeV, because of evaporation from the Sun, photinos *may* be responsible for significant fluxes of γ rays, positrons, or antiprotons and yet *not* give rise to an excessive flux of annihilation neutrinos. Such very light photinos, however, overclose the Universe since, for $m_S \gtrsim 60$ GeV, $\Omega_{\tilde{\gamma}}h_{1/2}{}^2 > 1$ (see Table VII and Fig. 4).

In summary, capture by the Sun and subsequent annihilation which results in high-energy (ordinary) neutrinos

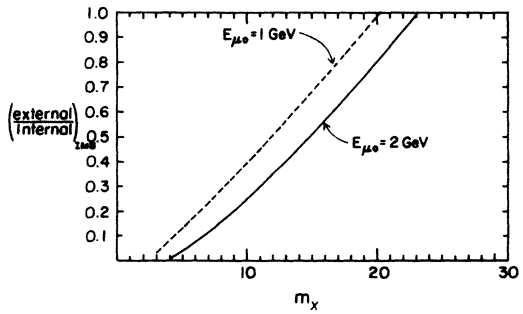

FIG. 9. The ratio of external (μ-induced) to internal (contained) events for the parameters of the IMB detector as a function of the photino mass for two choices of muon threshold energy.

TABLE VIII. Comparison of contained and external events from photinos with $\Omega_{\tilde{\gamma}}h_{1/2}{}^2=1$.

$m_{\tilde{\gamma}}$ (GeV)	$R_{\text{tot}}\times 3.3$ kt (yr^{-1})	R_μ (yr^{-1})[a]
3	35	0.07
4	27	0.4
8	14	2.3
12	9.1	3.5
16	6.3	4
20	4.7	4
24	3.6	4
28	2.9	4
32	2.3	4
36	1.9	4
40	1.7	4
50	1.2	3.5

[a]External events with a muon energy threshold of 2 GeV.

TABLE IX. Relic photino density and photino event rates for several choices of $m_{\tilde{\gamma}}$ and m_S.

$m_{\tilde{\gamma}}$ (GeV)	m_S (GeV)	$\Omega_{\tilde{\gamma}}^2 h_{1/2}^2$	R_{tot}
3	50[a]	0.87	15
	75	3.9	3.0
	100	11	0.9
4	50	0.53	17
	75	2.3	3.3
	100	6.6	1.1
8	50	0.23	22
	75	1.0	4.4
	100	2.9	1.4
15[b]	30	0.020	120
20[b]	25	0.011	130

[a]Silk and Srednicki (Ref. 1) for $\bar{p}$.
[b]Stecker, Rudaz, and Walsh (Ref. 26) for $\bar{p}$.

detectable in underground experiments provides significant constraints on WIMP candidates for the dark matter in the halo of the Galaxy. Dirac neutrinos can most likely be ruled out as cold-dark-matter candidates since, for those masses for which they are dynamically significant, the predicted event rate is large (for $m_{\nu_D} \approx 3.6$–15 GeV, $R_{\text{tot}} \approx 7$–17 events per kiloton year). Similarly, dynamically important Majorana neutrinos ($m_{\nu_D} \approx 5$–27 GeV) would result in $R_{\text{tot}} \approx 5$ events per kiloton year. In any case, such massive neutrinos are not expected to be stable on cosmological time scales.

Scalar neutrinos are possible cold-dark-matter candidates provided that various model-dependent parameters can be tuned to ensure a significant abundance of relic scalar neutrinos. Such cosmologically interesting scalar neutrinos would, however, give rise to an enormous flux of annihilation neutrinos provided that $m_{\tilde{\nu}} \gtrsim 2.8$ GeV.

Of the WIMP's we have considered, photinos are the remaining, potentially viable, candidates for the dark matter in the Universe. Although very light ($m_{\tilde{\gamma}} \lesssim 2.9$ GeV) photinos are not subject to the constraints from the underground detectors, they would overclose the Universe if $m_S \gtrsim 60$ GeV, as is suggested by accelerator data[22] (see Fig. 4). The combined constraints from the expected event rate and the universal mass density may be used to exclude significant regions in the $m_{\tilde{\gamma}}$ vs m_S plane (see Fig. 7). Only relatively high-mass photinos ($\gtrsim 25$ GeV) seem capable of escaping these constraints (see Fig. 7). The door is slowly closing on several cold-dark-matter candidates.

ACKNOWLEDGMENTS

We are grateful for helpful conversations with many people and, are especially indebted to K. Freese, G. Gelmini, M. W. Goodman, G. L. Kane, E. W. Kolb, L. M. Krauss, J. LoSecco, H. Meyer, K. A. Olive, W. H. Press, S. Rudaz, D. Seckel, D. N. Spergel, M. Srednicki, and J. van der Velde. We are especially grateful to D. Seckel for pointing out the correct form of the propagator factor in Eqs. (36) and (41) which led to the revision of Figs. 2, 3, and 4, and Tables I and IV as compared to the unpublished version. This work was supported in part by the U.S. Department of Energy under Contract No. DE-AC02-78ER05007.

[1]J. Silk and M. Srednicki, Phys. Rev. Lett. **53**, 624 (1984); J. Silk, K. A. Olive, and M. Srednicki, *ibid.* **55**, 257 (1985); J. S. Hagelin and G. L. Kane, Nucl. Phys. **B263**, 399 (1986).

[2]D. N. Spergel and W. H. Press, Astrophys. J. **294**, 663 (1985); W. H. Press and D. N. Spergel, *ibid.* **296**, 679 (1985).

[3]K. Freese, Phys. Lett. **167B**, 295 (1986); L. M. Krauss, M. Srednicki, and F. Wilczek, Phys. Rev. D **33**, 2079 (1986).

[4]T. K. Gaisser, T. Stanev, S. A. Bludman, and H. Lee, Phys. Rev. Lett. **51**, 223 (1983).

[5]Ya. B. Zeldovich, Adv. Astron. Astrophys. **3**, 241 (1965); H. Y. Chui, Phys. Rev. Lett. **17**, 712 (1966); G. Steigman, Annu. Rev. Nucl. Part. Sci. **29**, 313 (1979).

[6]R. J. Scherrer and M. S. Turner, Phys. Rev. D **33**, 1585 (1986).

[7]J. Ellis, J. S. Hagelin, D. V. Nanopoulos, K. A. Olive, and M. Srednicki, Nucl. Phys. **B238**, 453 (1984); E. W. Kolb and K. A. Olive, Phys. Rev. D **33**, 1202 (1986).

[8]J. Yang, M. S. Turner, G. Steigman, D. N. Schramm, and K. A. Olive, Astrophys. J. **281**, 413 (1984); A. M. Boegsgaard and G. Steigman, Annu. Rev. Astron. Astrophys. **23**, 319 (1985).

[9]D. Lynden-Bell, Mon. Not. R. Astron. Soc. **136**, 101 (1967).

[10]A. G. W. Cameron, in *Essays in Nuclear Astrophysics*, edited by C. A. Barnes, D. D. Clayton, and D. N. Schramm (Cambridge University Press, Cambridge, England, 1983), p. 23.

[11]G. Steigman, C. Sarazin, H. Quintana, and J. Faulkner, Astron. J. **83**, 1050 (1978).

[12]K. Shubert, in *Neutrino '84*, proceedings of the 11th International Conference on Neutrino Physics and Astrophysics, Dortmund, 1984, edited by K. Kleinknecht and E. A. Paschos (World Scientific, Singapore, 1984), p. 670.

[13]N. Cabibbo, G. Corbo, and L. Maiani, Nucl. Phys. **B155**, 93 (1979); G. Altarelli, N. Cabibbo, G. Corbo, L. Maiani, and G.

Martinelli, *ibid.* **B208**, 365 (1982).
[14]J. D. Bjorken and C. H. Llewellyn-Smith, Phys. Rev. D **7**, 887 (1973); C. H. Albright and C. Jarlskog, Nucl. Phys. **B84**, 467 (1975).
[15]G. L. Kane and I. Kani, UM Report No. TH 85-20, 1985 (unpublished).
[16]L. M. Krauss, K. Freese, D. N. Spergel, and W. H. Press, Astrophys. J. **299**, 1001 (1985).
[17]M. W. Goodman and E. Witten, Phys. Rev. D **31**, 3059 (1985).
[18]S. Z. Tilav, University of Delaware, M.Sc. thesis, 1986.
[19]E. W. Kolb and K. A. Olive, Phys. Rev. D **33**, 1202 (1986); M. Srednicki, K. A. Olive, and J. Silk, Report No. UMN-TH-553/86, 1986 (unpublished).
[20]J. S. Hagelin, G. L. Kane, and S. Raby, Nucl. Phys. **B241**, 638 (1984); L. E. Ibanez, Phys. Lett. **137B**, 160 (1984); see also J. S. Hagelin and G. L. Kane, Ref. 1.
[21]H. Goldberg, Phys. Rev. Lett. **50**, 1419 (1983); J. S. Hagelin, G. L. Kane, and S. Raby, Nucl. Phys. **B241**, 638 (1984).
[22]R. M. Barnett, H. E. Haber, and G. L. Kane, Nucl. Phys. **B267**, 625 (1986).
[23]J. M. Levy, in *Moriond Workshop on Massive Neutrinos in Astrophysics and in Particle Physics,* edited by J. Tran Thanh Van (Editions Frontières, France, 1984), p. 217.
[24]T. K. Gaisser and Todor Stanev, Phys. Rev. D **31**, 2770 (1985).
[25]T. K. Gaisser and Todor Stanev, Phys. Rev. D **30**, 985 (1984).
[26]J. Silk and M. Srednicki, Phys. Rev. Lett. **53**, 624 (1984); F. W. Stecker, S. Rudaz, and T. F. Walsh, *ibid.* **55**, 2622 (1985); J. S. Hagelin and G. L. Kane, Nucl. Phys. **B263**, 399 (1986).
[27]A. Buffington, S. Schindler, and C. Pennypacker, Astrophys. J. **248**, 1179 (1981).